Turkish Journal of Computer and Mathematics Education Vol.12 No.10 (2021), 2476-2488

Research Article

Medical Image Segmentation And Classification On Efficiently Fused Image Using Fast Fuzzy C Means Algorithm And Convolutional Neural Network

V. Amala Rani[1], Dr.S. Lalithakumari[2]

[1]Research Scholar, School of Electrical and Electronics, Sathyabama Institute of Science and Technology, Chennai.
[2]Department of Electronics & Instrumentation, Sathyabama Institute of Science and Technology, Chennai.

Article History: Received: 10 January 2021; Revised: 12 February 2021; Accepted: 27 March 2021; Published online: 28 April 2021

Abstract: In the recent past, medical image processing plays significant role in diagnosis of disease using Computer Aided Diagnosis (CAD). In this research, we propose a novel approach for classification of medical images using Fast Fuzzy C-Means (FFCM) clustering and Convolutional Neural Networks (CNN). Initially, the images were pre-processed using filtering and enhancement techniques. Image filtering was performed using 2D Gabor Filter. This step helped to remove noise in the medical data. Then, image enhancement was performed using Edge Preservation-Contrast Limited Adaptive Histogram Equalization (EP-CLAHE) technique. Fusion of medical data belonging to different modality results in the generation of a single image that has extended information content and helps to increase the reliability of disease diagnosis. The images were fused using 2-Dimensional Double Density Wavelet Transform (2D-DDWT) and Empirical Principle Component Analysis (EPCA). Segmentation plays a crucial role in detecting tumor cells in medical images. Here, segmentation was performed using FFCM clustering algorithm. The FFCM clustering helps in achieving accurate segmentation results with reduced computational complexity. The efficiency and reliability of a classification algorithm depend on the type of features extracted from the classification data. In our research, Gray Level Co-Occurrence Matrix (GLCM) features were extracted from the segmented data. Deep Learning (DP) technique is widely used for classification of image using significant features with high accuracy and efficiency. Using these features, classification was performed using CNN. The images were classified into benign and malignant. The simulation was performed using publicly available datasets. The outcome of the research shows that the proposed scheme was very effective in the classification of tumor images. The classification performance of the proposed framework was validated using metrics like recall, precision, specificity, F-score and accuracy. Experimental results demonstrate the credibility of the proposed framework and prove that the proposed scheme outperforms state-of-the-art works in the research.

Keywords: 2D-Gabor Filter, EP-CLAHE, FFCM, GLCM, CNN.

1. Introduction

Early diagnosis of brain tumour is vital as it aids in early treatment and complete recovery of patients[1].Computer Aided Diagnosis (CAD) is widely being used recently for discerning brain tumor images into benign and the malignant cases[2]. These techniques are based on two types of images namely the magnetic resonance imaging (MRI)[3][4][5][6] and computed tomography (CT)[7][8][9][10] images. These brain images comprise of both normal and abnormal cases. Development of automatic classification tool using these images as inputs aids the physicians in early detection of the disease and successful treatment. The main steps involved in this classification include image pre-processing, feature extraction and classification. Several classifiers like AdaBoost classifier[11], support vector machine (SVM)[12], least square SVM[13] and deep learning techniques[14][15] have been employed in the literature for medical image classification. Recently Convolutional Neural Networks[16][17] are widely being used for classification of brain images due to their reliability. Accurate classification of these images is difficult due to factors like variation in size, texture, shape, intensity values, etc. To achieve good classification results in our work we have proposed novel image enhancement technique using EP-CLAHE. To further improve the accuracy of classification, in our work we have first fused both the MRI and CT images and then employed the fused image for classification. Features are derived from the fused image and classification is done using CNN algorithm.

The remainder of the paper is organized as follows. Section 2 includes a detailed literature survey of the previous works in the literature. Section 3 describes the proposed methodology. The results and discussion are performed in Section 4. Conclusion of the paper is given in Section 5.

2. Literature survey

A method for the diagnosis of brain tumor using MRI images was proposed in [18]. In this paper a technique for the identification of Alzheimer's disease was given. The framework comprised of four steps. The first step was MRI image acquisition. The second step was pre-processing of MRI data. The third step was extraction of features. The final step was classification. Classification of brain tumor based on CNN features was proposed in [19]. Here

the data was classified into three different classes. They were the glioma, meningioma and the pituitary tumors. In this paper, feature extraction was done using GoogLeNet. This system achieved a high overall classification accuracy of about 98%. The authors of [20] proposed a technique for brain tumor identification using transfer learning. This system utilized pre-trained Convolutional Neural Network framework. In this paper, a new fine-tuning technique was utilized. This system achieved an overall accuracy of about 94.82%. Testing based on five-fold validation was used in this paper. Texture and shape features were employed for the classification of MRI images in [21]. Here the entire framework comprised of four main sequential steps. Initially, the region of interest (ROI) was identified. In the next step, features were extracted from the defined ROI. In the third step, from the extracted features few important features were selected. In the final step, classification was performed. A technique for the identification of abnormality in the brain tumor based on k-means clustering was proposed in [22]. Here, Artificial Neural Networks (ANN) was employed for identification of tumor region in the MRI data. A new technique for the identification of region with tumor cells from the MRI images was proposed in this paper. Classification of tumor images using hybrid feature extraction technique was proposed in [23]. This paper utilized Extreme Learning Machine for classification. Features were extracted from the region of interest using hybrid feature extraction technique. These features were then used for the computation of a covariance matrix. From the matrix, principal component analysis was done for projection of data. Score level fusion was employed for the classification of brain images in[24]. Spatial domain technique was employed in this paper for the classification using transfer learning. The final classification was done by employing a SoftMax layer. A framework based on feature enhancement for tumor image classification was presented in [25]. Here, analysis was done on various pre-processing techniques applied before the classification of MRI images. They were categorized into three different groups. The first group was the noise removal group. The second group comprised of the papers related to contrast enhancement. The third group comprised of the edge detection group. CNN was employed in brain tumor classification in [26]. Small kernels were employed for the formation of deep architectures. Also, smaller weights were assigned for each neuron units. This system achieved an overall classification accuracy of about 97.5%. Also, the computational complexity of this system was too low. A new genetic technique was used for the identification of brain tumor in [27]. Here, various segmentation techniques were analyzed and compared in this paper. The genetic algorithm employed in this paper comprised of area calculation. This system achieved an overall classification accuracy of about 93.79%. A survey on brain tumor image classification was presented in [28]. Various methods proposed so far for the segmentation of tumor regions from MRI data were analyzed and compared in this paper. In addition, various classification techniques for tumor diagnosis proposed in the system were also analyzed in this paper. Detection of tumor region using a k-means clustering and ANN was presented in [29]. In this paper, feature extraction was performed using GLCM. Using these features, Fuzzy system was developed. The next step was thresholding. Then the morphological operator was applied. Finally, the tumor region was segmented. Detection of brain tumor using DWT fusion was presented in [30]. This fusion was used for the combination of two types of information namely the texture and the structural details of the MRI data. The fusion process was followed by noise removal system using a diffusion filter. Then thresholding was done for ROI segmentation. Finally, classification was done using CNN. The authors of [31] presented a framework for the tumor segmentation using CNN algorithm. A deep convolution neural network was employed in this paper. All the network layers were arranged in the form of a sequential order for classification. A new approach were employed for classifying tumor images in [32]. In this paper, Support Vector Machine was employed for classification. Features like texture, intensity and shape were employed in this paper. This paper achieved an accuracy of 97.1%.Probabilistic neural networks were employed for tumor detection in [33]. Here the MRI images were categorized into three categories. The first category was normal. The second was benign and the third was malignant. Here GLCM features were extracted from the images. Compression was performed using principal component analysis. Wavelet transform-based tumor classification system was presented in [34]. Here the data was first pre-processed using anisotropic diffusion filter. Then, DWT features were derived. Finally, classification was done using SVM. Classification of MRI images using AdaBoost classification was presented in [35]. Initially data was pre-processed for noise removal. Then GLCM features were extracted. Finally, the classification was performed using the AdaBoost classifier.

3. Proposed Methodology

The proposed methodology comprises of steps like image preprocessing (filtering and enhancement), fusion, ROI region segmentation, extraction of relevant features and final classification.This is depicted in Figure 1. The noisy MRI and noisy CT images are first obtained. These data are pre-processed using filtering and enhancement. Filtering is done to remove noise and enhancement is done to increase the contrast of the image. These noiseless images are then combined to form an image using image fusion. Then from the fused image, the region of interest

(ROI) is segmented using image segmentation. Then, from the segmented regions, the features are extracted and finally the fused image is classified to two cases, benign and malignant.

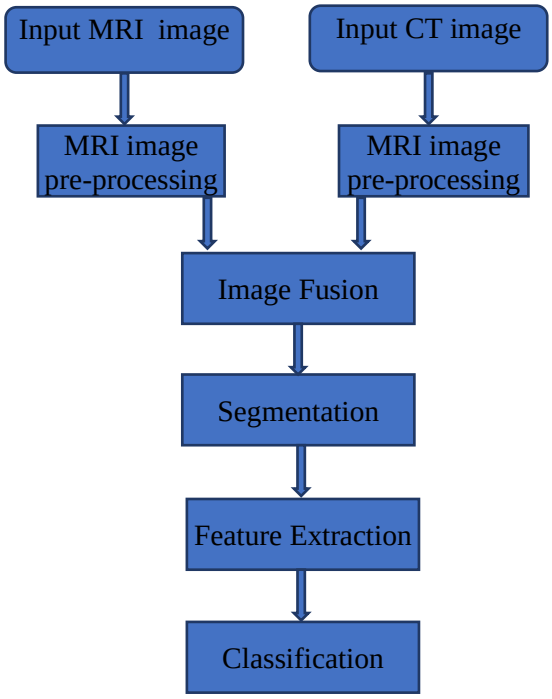

Figure 1. Flow chart of proposed methodology

3.1. Image Preprocessing

The first step was performed in two levels namely, filtering and enhancement. Image filtering was performed using 2D Gabor filter and enhancement was performed using a novel Edge Preservation-based Contrast Limited Adaptive Histogram Equalization technique.

3.1.1. Image Filtering

The input images $I \in R^{M \times N}$ were first filtered using 2D Gabor filters. In this filtering technique, the image $I(m,n)$ is convolved using Gabor function $u(m,n)$ using the following equation

$$u(m,n) = \iint_{\Omega} I(\xi,\eta) g(m-\xi, n-\eta) d\xi d\eta \quad (1)$$

In our work, we have employed Gabor function family as in[36]. It is defined as follows

$$g_{\lambda,\theta,\phi}(m,n) = e^{-((m'^2+\gamma^2 n'^2)/2\sigma^2)} \cos(2\Pi \frac{m'}{\lambda} + \phi) \quad (2)$$

Here, $m' = m\cos\theta + n\sin\theta, n' = -m\sin\theta + n\cos\theta$, $\sigma = 0.56\lambda$ and $\gamma = 0.5$ .Here, σ represents the scaling factor and θ represents the orientations of the filter functions. Thus, filtered images $I^F \in R^{M \times N}$ were obtained by convolving input images with the Gabor function defined in Equation (2).

3.1.2. Image Enhancement

The filtered images were then enhanced using a novel Edge Preservation-based Contrast Limited Adaptive Histogram Equalization technique. This technique is given in Algorithm 1. The main objective of this algorithm is to preserve the edge information in the images. Since the adaptive histogram equalization technique equalizes the histogram of an image in a uniform manner, the edge information gets degraded. To avoid this, in the proposed algorithm we have initially identified the regions containing edges. The histogram equalization is not applied for the edge regions. That is, the entire image is first divided into four groups namely, the edge blocks, corner blocks, border blocks and the internal smooth blocks. To preserve the edge and corner details, the edge, corner and border blocks are retained. The histogram equalization is applied only for the internal smooth blocks.

Algorithm 1: Proposed Edge Preservation-based Contrast Limited Adaptive Histogram Equalization (EP-CLAHE) technique.

Input:

Filtered image $I^F \in R^{M\times N}$.

Output:

Enhanced image $I^E \in R^{M\times N}$.

Steps:

1 Obtain the edge map $I^{EM} \in R^{M\times N}$ of the image $I^F \in R^{M\times N}$ using Canny edge detector.

2 Divide the entire image I^F into non-overlapping blocks of size $n\times n$.

3 From the edge map I^{EM}, identify the blocks that comprises of edge pixels as Edge Blocks (*EB*).

4 Identify the four corner blocks as Corner Blocks (*CB*).

5 The border blocks other than the four corner blocks are identified as Border Blocks (BB).

6 The remaining blocks are identified as the Inner Smooth Blocks (ISB).

7 Compute the histogram of each region.

8 Obtain uniform density function for the ISB regions by computing the CDF[37] of the histogram using,

$$C_{i,j}(n) = \frac{(N-1)}{M}\sum_{k=0}^{n} h_{i,j}(k) \;\; ; n = 1, 2, ..., N-1.$$

9 Map every pixel in the ISB block by linear combination of results obtained from four nearest regions to obtain the Enhanced image $I^E \in R^{M\times N}$.

3.2. Image Fusion

The enhanced MRI and CT images are fused using the Empirical Principle Component Analysis-based2-Dimensional Double Density Wavelet Transform (2DDDWTEPCA) technique. Here, the input MRI and CT images are initially decomposed into 9 sub-bands using 2D Double Density Wavelet Transform. These sub-bands are divided into three groups, namely, the sub-bands with low frequency, sub-bands with high frequency and the sub-bands with mixed frequency. The sub-bands having low frequency include the LL sub-bands. The sub-bands with high frequency include the $H_1H_1, H_1H_2, H_2H_1 \text{ and } H_2H_2$ sub-bands. The sub-bands having mixed-frequency include the $LH_1, LH_2, H_1 \text{ and } H_2L$ sub-bands. In our proposed algorithm, these three groups are fused using weighted fusion technique. However, the weights for the fusion is computed differently for the three groups. The weights for the fusion of low frequency region is based on the entropy. Entropy is chosen as it represents the information content of the regions. The high frequency sub-bands are fused using standard deviation as the weights. This is because, the high frequency regions contain the edge information. Hence, more priority is given for regions having more edge features. Finally, the mixed frequency regions are fused based on Empirical Principal Component Analysis (PCA) technique. In this technique, the covariance matrix is first computed. Then the eigen vector corresponding to the largest eigen value is chosen. Finally, fusion is done based on the values of the eigen vectors.

3.3. Tumor Segmentation

Tumor region segmentation is performed using clustering and thresholding techniques.

3.3.1. Fast Fuzzy C Means Clustering (FFCMC)

FCMC[38] is a popular method used in segmenting images since the efficiency of this algorithm is better than other machine learning techniques. However, the main drawback of this technique was the speed. To improve the speed of this algorithm, FFCMC algorithm was used. In this algorithm, the main difference was that, image histogram was used instead of raw image pixels. Here, the objective function of FFCMC is given by,

$$J = \sum_{i=0}^{255}\sum_{q=1}^{C} h_i f_{iq} d(i, \theta_q) \tag{3}$$

Here, h_i refers to the histogram,

f_{iq} refers to the fuzzy membership between pixel x_i and histogram of cluster with center θ_q,

$d(i, \theta_q)$ refers to the distance between pixel x_i and histogram of cluster with center θ_q.

3.3.2. Otsu Thresholding

Otsu threshold [39] is a widely used threshold for creating segmented regions in images. It identifies a global threshold for segmenting an image into two categories namely, the foreground and the background. Using the threshold value each pixel is classified to two categories. If the value of the pixel is greater than the threshold, then it is classified as foreground, else it is classified as a background pixel.

3.4. Feature Extraction

In this work, we have extracted GLCM features [40].This feature exploits the special relationship between two pixels that are spaced by a particular distance in an image. The GLCM feature has a rapidly changing value in fine texture regions and a slowly changing value in the coarse texture regions. It is computed as

$$G(m,n) = \frac{\#\{[(m_1,n_1),(m_2,n_2)] \in S \mid f(m_1,n_1) = g_1 \,\&\, f(m_2,n_2) = g_2\}}{\#S} \tag{4}$$

Using this technique several statistical features like contrast, energy, homogeneity, correlation was extracted.

Angular second moment:

Angular second moment represents the uniformity of the distribution of the image. It is computed using the following formula

$$A_{sm} = \sum_{m}^{M}\sum_{n}^{N} G(m,n)^2 \tag{5}$$

Correlation:

Correlation value indicates the similarity of the texture of the image in the two perpendicular directions namely, the horizontal and the vertical directions. It is computed using

$$C_{or} = \frac{\sum_{m}^{M}\sum_{n}^{N}(m-\bar{x})(n-\bar{y})G(m,n)}{\sigma_x \sigma_y} \tag{6}$$

Contrast:

Contrast value indicates the variation of depth and smooth regions of the image and is computed as

$$C_{on} = \sum_{m}^{M}\sum_{n}^{N}(m-n)^2 G(m,n) \tag{7}$$

Entropy:

Entropy is the measure of information content and is computed using

$$E_{nt} = -\sum_{m}^{M}\sum_{n}^{N} G(m,n) I_g G(m,n) \tag{8}$$

3.5. Classification

The above-mentioned features are computed from the segmented regions. These features are extracted from both the benign and malignant images. From these training features classification models are created during the training phase. Using the classification model classification is done during testing. In our work, we have employed the Convolutional Neural Networks (CNN) for classification of tumor images.

The network architecture comprises of input block, output block, main block and classification block. The main block comprises of two internal blocks. The input image is acquired in the input block. The first internal block comprises of three layers. A convolutional layer is used as a first layer. This layer is followed by an activation layer. The third layer is a dropout layer. The activation layer being used is rectified linear unit. The first internal block output has a size that is twice smaller than that of the input. The output of this layer is given as input to the second internal block. This layer is similar to the first internal block. It comprises of convolutional layer, activation later and a dropout layer. The final classification takes places at the classification block. It has two fully connected layers. The final output of this block is either "1" that represents benign or "2" that represents malignant.

4. Results and Discussion

4.1. Parameter Settings

The proposed system was simulated using MATLAB software running on windows intel i3 core processor with 6GB RAM. Four pairs of MRI and CT images were considered for analysis on our work.

4.2. Simulation Results

Figure 2 shows the input noisy MRI images. This image has noise and hence cannot be processed directly. Similarly, Figure 3 shows the input noisy CT images.

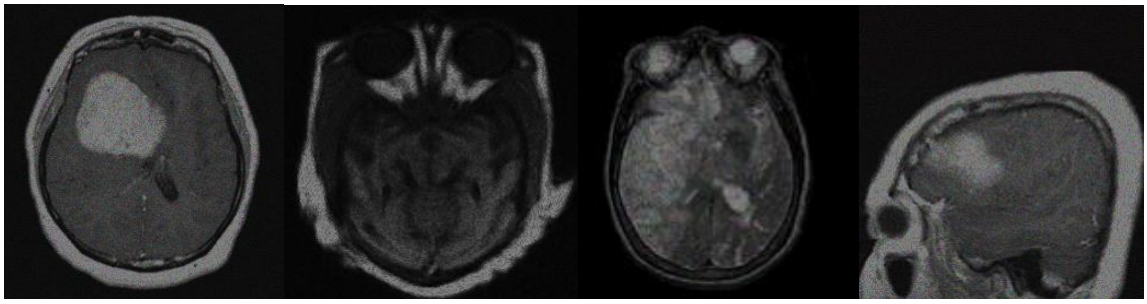

Figure 2. Input noisy MRI images

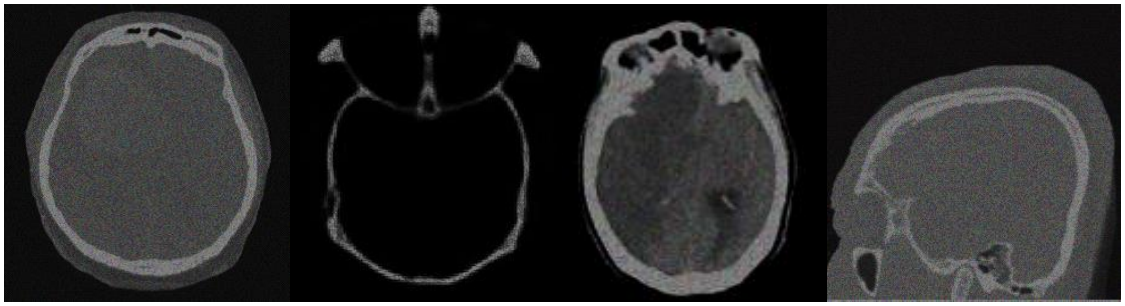

Figure 3. Input noisy CT images

Figure 4 shows MRI images that are filtered using Gabor filter. From Figure 4 we infer that the filtered images have less noise compared to the original images. Similarly, Figure 5 shows the 2D Gabor filtered CT images.

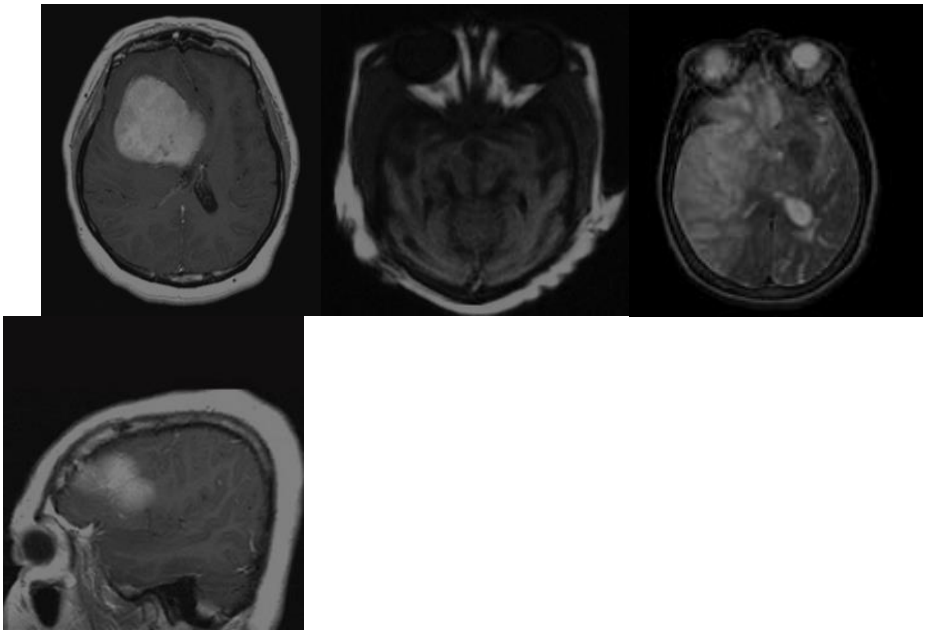

Figure 4. 2D Gabor filtered MRI images

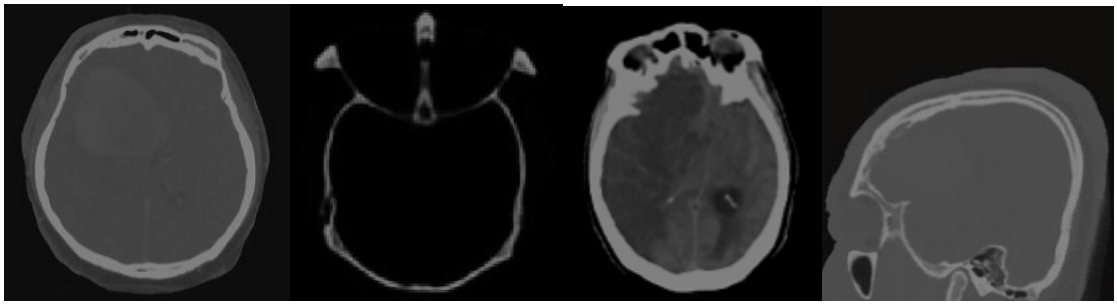

Figure 5. 2D Gabor filtered CT images

Figure 6 shows EP-CLAHE MRI enhanced images. Similarly, Figure 7 shows EP-CLAHE CT enhanced images. From Figure 6 and Figure 7, it is obvious that the enhanced images have better clarity and contrast compared to the original images.

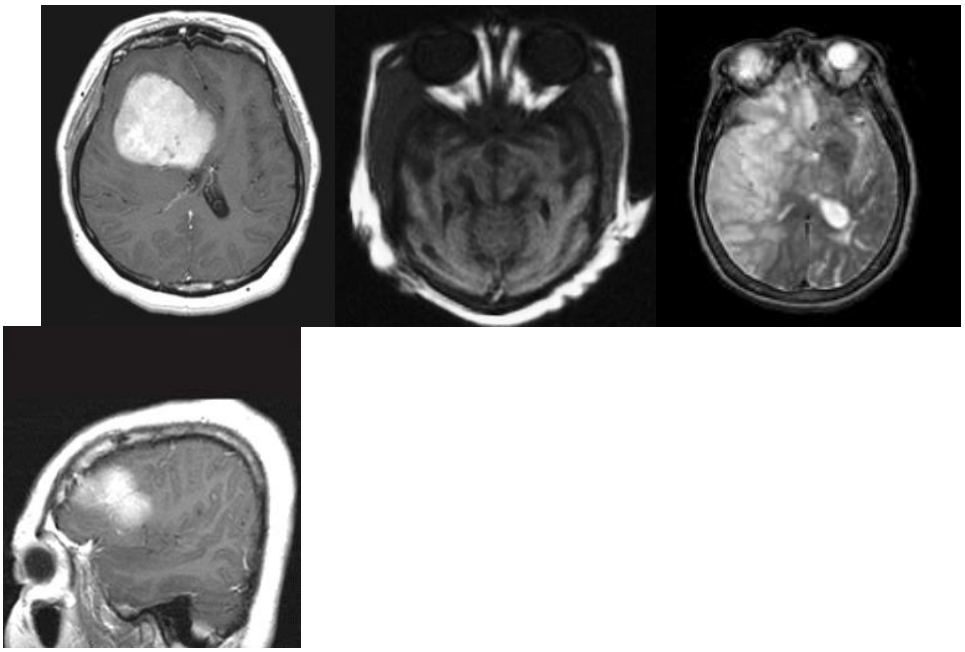

Figure 6. EP-CLAHE enhanced MRI images

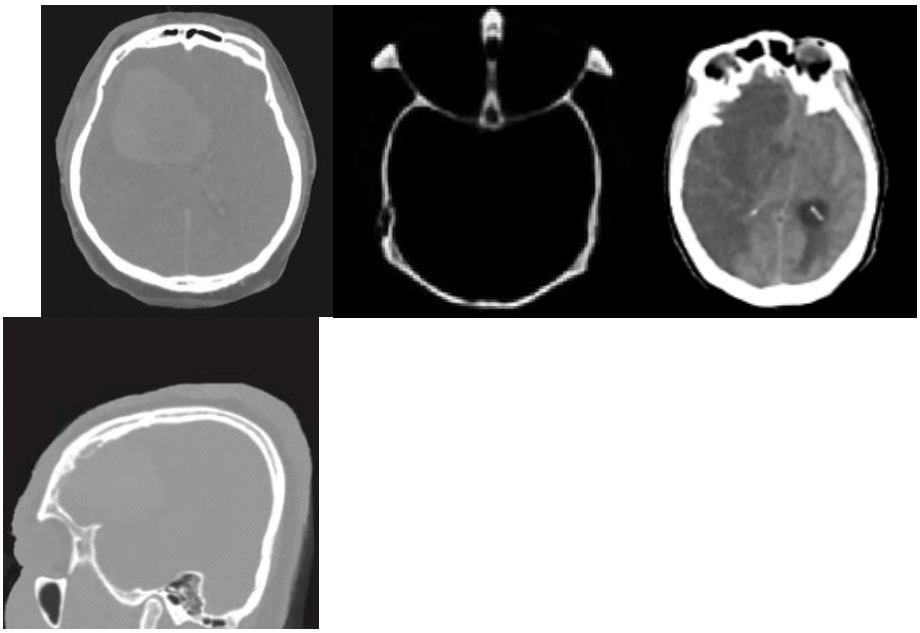

Figure 7. EP-CLAHE enhanced CT images

Figure 8 shows normal and abnormal image segmentation results using FFCM algorithm. The segmentation results clearly show the regions containing the tumor cells. From these segmented regions, the features are extracted.

Figure 8. Normal and abnormal image segmentation using FFCM.

4.3. Quantitative Analysis

4.3.1. SegmentationTechnique Evaluation

Jaccard coefficient (JC) is commonly used for evaluating the performance of segmentation algorithms. It is given by

$$J(O_a) = \frac{B \cap G}{B \cup G} \tag{15}$$

where O_a is the overlap area, B refers to the binary image and G refers to the ground truth image.

The Dice coefficient (DC) is computed as

$$D(B,G) = \frac{2|B \cap G|}{|B| + |G|} \tag{16}$$

Its value ranges between 0 to 1. A value of 0 indicates that there is no overlap and 1 show that there is full overlap.

Table 1` shows the performance evaluation using Jaccard Coefficient. From Table 1 we infer that, the average value of JC for K means clustering was 0.5068. Similarly, the average value of JC for Fuzzy C Means Clustering was 0.6195. But Fast Fuzzy C Means Clustering achieved a maximum Jaccard Coefficient of 0.7383. Thus, our proposed framework achieves best performance in terms of Jaccard Coefficient.

Table 1. Performance evaluation using Jaccard Coefficient

Image Set	**Jaccard Coefficient**		
	K means clustering	Fuzzy C Means Clustering	Fast Fuzzy C Means Clustering
1	0.55869	0.5979	0.7129
2	0.4632	0.5980	0.7549
3	0.5122	0.6136	0.7618
4	0.4933	0.6688	0.7239

Table2 shows the performance evaluation using Dice Coefficient. From Table 6 we infer that, the average value of Dice Coefficient for K means clustering was 0.6209. Similarly, the average value of DC for Fuzzy C Means Clustering was 0.6685. But FFCMC achieved a maximum DC of 0.7768. Thus, our proposed framework achieves best performance in terms of DC.

Table 2. Performance evaluation using Dice Coefficient

Image Set	Dice Coefficient		
	K means clustering	Fuzzy C Means Clustering	Fast Fuzzy C Means Clustering
1	0.6192	0.6518	0.7723
2	0.6209	0.6611	0.7312
3	0.6287	0.6691	0.8126
4	0.6151	0.6922	0.7911

4.3.2. Evaluation of Classification Algorithms

To evaluate the classification performance, metrics like overall accuracy, recall, precision, specificity and F-score were employed.

Overall accuracy (O_a):

Overall accuracy indicates the overall classification performance of the classifier.

$$O_a = \frac{TP + TN}{TP + TN + FP + FN} \tag{21}$$

Recall (R_e):

The recall refers to the sensitivity of classification and is computed as

$$R_e = \frac{TP}{TP + FN} \tag{22}$$

Precision (P_r):

The precisionis the ratio of number of true positives to the sum of true positives and false positives.

$$P_r = \frac{TP}{TP + FP} \tag{23}$$

Specificity(S_p):

The specificityis the ratio of number of true negatives to the sum of true negatives and false positives.

$$S_p = \frac{TN}{TN + FP} \tag{24}$$

F-score (F_s):

The F-score is computes as

$$F_s = 2 \times \frac{Precision \times Recall}{Precision + Recall} \tag{25}$$

The classification is also performed using traditional algorithms like k-nearest neighbour (k-NN), Naïve Bayes, Random Forest, support vector machine (SVM) for comparison. Table 7 shows the results obtained in terms of overall accuracy. From Table 3, we see that CNN algorithm produces the best results compared to all other traditional classification algorithms.

Table 3. Comparison of Overall Accuracy

Classification algorithms	Overall accuracy (%)			
	IS 1	**IS 2**	**IS 3**	**IS 4**
k-NN	90.23	90.52	91.23	92.53
Naïve Bayes	91.92	90.23	92.42	92.56
Random Forest	92.43	93.24	93.72	92.83

SVM	93.12	93.75	93.83	94.66
CNN	**95.82**	**96.83**	**95.15**	**96.73**

Figure 9represents the comparison of specificity for the four image sets. Form Figure 9 we see that the average value of specificity obtained by k-NN, Naïve Bayes, Random Forest, SVM and CNN are 94.75, 96.07, 96.77, 98.08 and 98.99 respectively. Thus, it is clearly seen that CNN outperforms other algorithms.

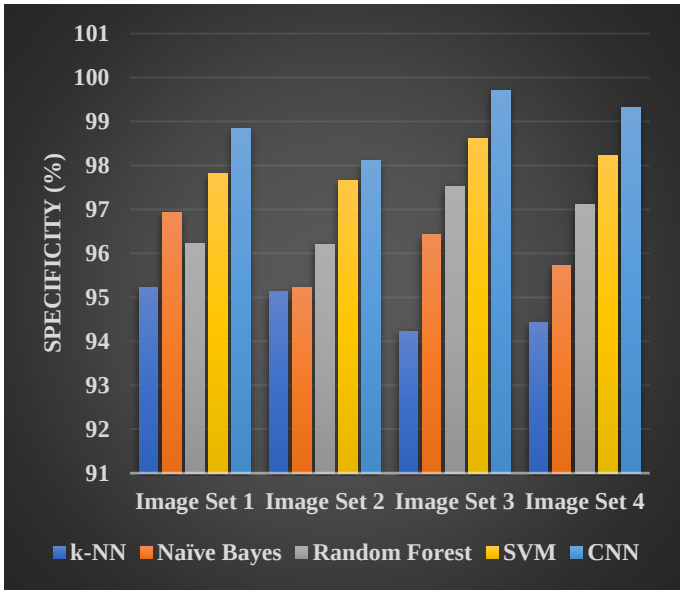

Figure 9. Comparison of specificity

Figure 10 represents the comparison of precision for the four image sets. Form Figure 10 we see that the average value of precision obtained by k-NN, Naïve Bayes, Random Forest, SVM and CNN are 89.42, 92.31, 93.31, 94.41 and 96.37 respectively. Thus, it is clearly seen that CNN is the best compared to other algorithms.

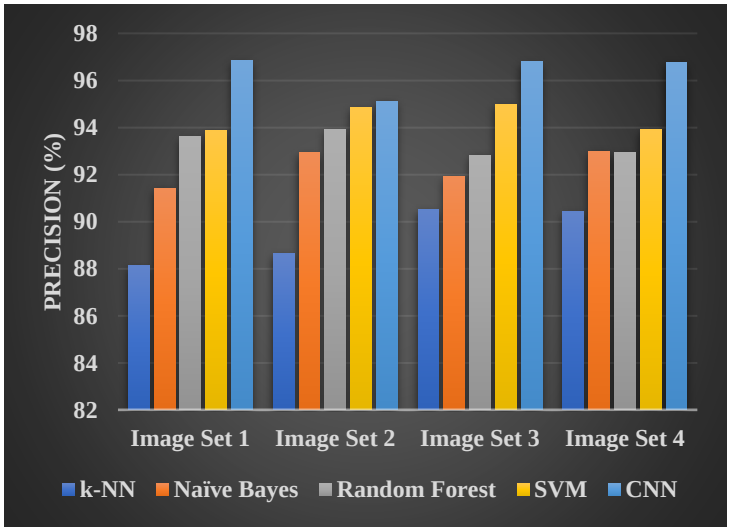

Figure 10. Comparison of precision

Figure 11 represents the comparison of recall for the four image sets. Form Figure 11 we see that the average value of recall obtained by k-NN, Naïve Bayes, Random Forest, SVM and CNN are 90.50, 92.07, 93.02, 93.60 and 94.99 respectively. Thus, it is clearly seen that CNN performs better that other traditional classification algorithms.

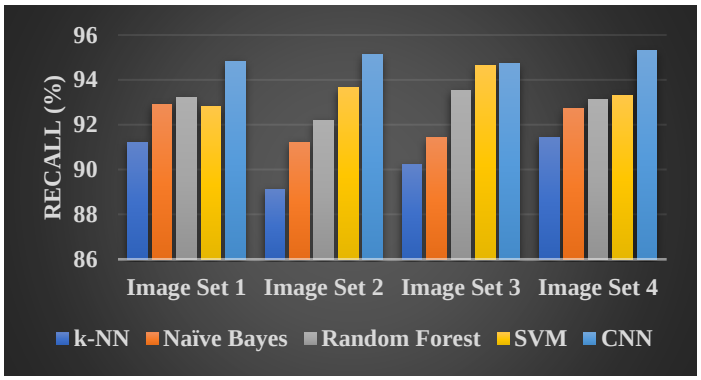

Figure 11. Comparison of recall

Figure 12 represents the comparison of F-score for the four image sets. Form Figure 12 we see that the average value of F-score obtained by k-NN, Naïve Bayes, Random Forest, SVM and CNN are 91.86, 92.78, 94.06, 94.13 and 96.43 respectively. Thus, the F-score of CNN is better than other algorithms.

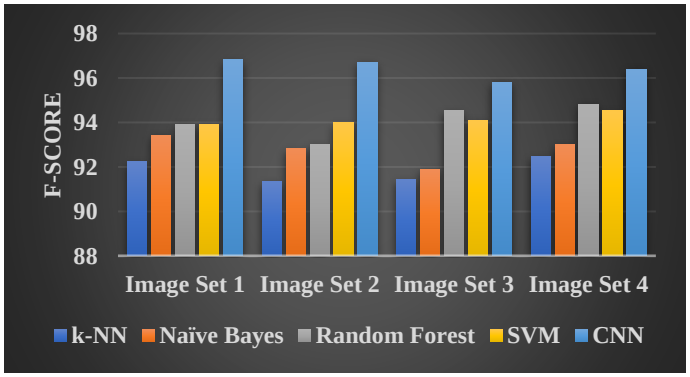

Figure 12. Comparison of F-score

5. Conclusion

In this research we proposed a novel approach for classification of medical images using FFCMC and CNN. Images were filtered using 2D Gabor filters. Then they were enhanced using Edge Preservation-CLAHE system. The MRI and CT images were then fused using 2-Dimensional Double Density Wavelet Transform and Empirical Principle Component Analysis. The fused images were segmented using FFCMCalgorithm. Then,GLCM features were extracted from the segmented data. Finally, classification was done using Convolutional Neural Networks. The proposed scheme produces excellent results in terms of quantitative analysis. Simulation was performed using four pairs of MRI and CT images. The credibility of the segmentation methodology was proved using Jaccard and Dice coefficients. It was observed that the Fuzzy Fast C Means Clustering algorithm achieved an average Jaccard and Dice coefficient values of 0.7383 and 0.7768 respectively. Finally, the CNN classification algorithm was compared with traditional machine learning algorithms like k-NN, Naïve Bayes, random forest and SVM. It was observed that CNN produced excellent results in terms of all the classification metrics.

References

1. E. A. S. El-Dahshan, H. M. Mohsen, K. Revett, and A. B. M. Salem, "Computer-aided diagnosis of human brain tumor through MRI: A survey and a new algorithm," *Expert Syst. Appl.*, vol. 41, no. 11, pp. 5526–5545, 2014.
2. S. Kumar, C. Dabas, and S. Godara, "Classification of Brain MRI Tumor Images: A Hybrid Approach," in *Procedia Computer Science*, 2017, vol. 122, pp. 510–517.
3. S. Pereira, A. Pinto, V. Alves, and C. A. Silva, "Brain Tumor Segmentation Using Convolutional Neural Networks in MRI Images," *IEEE Trans. Med. Imaging*, vol. 35, no. 5, pp. 1240–1251, 2016.
4. N. N. Gopal and M. Karnan, "Diagnose brain tumor through MRI using image processing clustering algorithms such as Fuzzy C Means along with intelligent optimization techniques," in *2010 IEEE International Conference on Computational Intelligence and Computing Research, ICCIC 2010*, 2010,

pp. 694–697.

5. H. Khotanlou, O. Colliot, J. Atif, and I. Bloch, "3D brain tumor segmentation in MRI using fuzzy classification, symmetry analysis and spatially constrained deformable models," *Fuzzy Sets Syst.*, vol. 160, no. 10, pp. 1457–1473, 2009.
6. P. Vasuda and S. Satheesh, "Improved Fuzzy C-Means Algorithm for MR Brain Image Segmentation," *Int. J. Comput. Sci. Eng.*, vol. 2, no. 5, pp. 1713–1715, 2010.
7. X. W. Gao, R. Hui, and Z. Tian, "Classification of CT brain images based on deep learning networks," *Comput. Methods Programs Biomed.*, vol. 138, pp. 49–56, 2017.
8. J. M. Wolterink, A. M. Dinkla, M. H. F. Savenije, P. R. Seevinck, C. A. T. van den Berg, and I. Išgum, "Deep MR to CT synthesis using unpaired data," in *Lecture Notes in Computer Science (including subseries Lecture Notes in Artificial Intelligence and Lecture Notes in Bioinformatics)*, 2017, vol. 10557 LNCS, pp. 14–23.
9. X. W. Gao and R. Hui, "A deep learning based approach to classification of CT brain images," in *Proceedings of 2016 SAI Computing Conference, SAI 2016*, 2016, pp. 28–31.
10. X. Han, "MR-based synthetic CT generation using a deep convolutional neural network method:," *Med. Phys.*, vol. 44, no. 4, pp. 1408–1419, 2017.
11. J. Jiang, Y. Wu, M. Huang, W. Yang, W. Chen, and Q. Feng, "3D brain tumor segmentation in multimodal MR images based on learning population- and patient-specific feature sets," *Comput. Med. Imaging Graph.*, vol. 37, no. 7–8, pp. 512–521, 2013.
12. U. Javed, M. M. Riaz, A. Ghafoor, and T. A. Cheema, "MRI brain classification using texture features, fuzzy weighting and support vector machine," *Prog. Electromagn. Res. B*, no. 53, pp. 53–73, 2013.
13. H. Selvaraj, S. T. Selvi, D. Selvathi, and L. Gewali, "Brain mri slices classification using least squares support vector machine," *IC-MED Int. J. Intell. Comput. Med. Sci. Image Process.*, vol. 1, no. 1, pp. 21–33, 2007.
14. M. Yousefi, A. Krzyżak, and C. Y. Suen, "Mass detection in digital breast tomosynthesis data using convolutional neural networks and multiple instance learning," *Comput. Biol. Med.*, vol. 96, pp. 283–293, 2018.
15. O. Charron, A. Lallement, D. Jarnet, V. Noblet, J. B. Clavier, and P. Meyer, "Automatic detection and segmentation of brain metastases on multimodal MR images with a deep convolutional neural network," *Comput. Biol. Med.*, vol. 95, pp. 43–54, 2018.
16. A. Işin, C. Direkoğlu, and M. Şah, "Review of MRI-based Brain Tumor Image Segmentation Using Deep Learning Methods," in *Procedia Computer Science*, 2016, vol. 102, pp. 317–324.
17. N. Abiwinanda, M. Hanif, S. T. Hesaputra, A. Handayani, and T. R. Mengko, "Brain tumor classification using convolutional neural network," in *IFMBE Proceedings*, 2019, vol. 68, no. 1, pp. 183–189.
18. B. F. Marghalani and M. Arif, "Automatic Classification of Brain Tumor and Alzheimer's Disease in MRI," *Procedia Comput. Sci.*, vol. 163, pp. 78–84, 2019.
19. S. Deepak and P. M. Ameer, "Brain tumor classification using deep CNN features via transfer learning," *Comput. Biol. Med.*, vol. 111, no. March, p. 103345, 2019.
20. Z. N. K. Swati *et al.*, "Brain tumor classification for MR images using transfer learning and fine-tuning," *Comput. Med. Imaging Graph.*, vol. 75, pp. 34–46, 2019.
21. E. I. Zacharaki *et al.*, "Classification of brain tumor type and grade using MRI texture and shape in a machine learning scheme," *Magn. Reson. Med.*, vol. 62, no. 6, pp. 1609–1618, 2009.
22. N. Arunkumar *et al.*, "K-Means clustering and neural network for object detecting and identifying abnormality of brain tumor," *Soft Comput.*, vol. 23, no. 19, pp. 9083–9096, 2019.
23. A. Gumaei, M. M. Hassan, M. R. Hassan, A. Alelaiwi, and G. Fortino, "A Hybrid Feature Extraction Method with Regularized Extreme Learning Machine for Brain Tumor Classification," *IEEE Access*, vol. 7, no. c, pp. 36266–36273, 2019.
24. J. Amin, M. Sharif, M. Yasmin, T. Saba, M. A. Anjum, and S. L. Fernandes, "A New Approach for Brain Tumor Segmentation and Classification Based on Score Level Fusion Using Transfer Learning," *J. Med. Syst.*, vol. 43, no. 11, 2019.
25. B. Tahir *et al.*, "Feature enhancement framework for brain tumor segmentation and classification," *Microsc. Res. Tech.*, vol. 82, no. 6, pp. 803–811, 2019.
26. J. Seetha and S. S. Raja, "Brain tumor classification using Convolutional Neural Networks," *Biomed. Pharmacol. J.*, vol. 11, no. 3, pp. 1457–1461, 2018.
27. N. B. Bahadure, A. K. Ray, and H. P. Thethi, "Comparative Approach of MRI-Based Brain Tumor Segmentation and Classification Using Genetic Algorithm," *J. Digit. Imaging*, vol. 31, no. 4, pp. 477–489, 2018.
28. G. Mohan and M. M. Subashini, "MRI based medical image analysis: Survey on brain tumor grade classification," *Biomed. Signal Process. Control*, vol. 39, pp. 139–161, 2018.

29. M. Sharma, G. N. Purohit, and S. Mukherjee, "Information Retrieves from Brain MRI Images for Tumor Detection Using Hybrid Technique K-means and Artificial Neural Network (KMANN)," pp. 145–157, 2018.
30. J. Amin, M. Sharif, N. Gul, M. Yasmin, and S. A. Shad, "Brain tumor classification based on DWT fusion of MRI sequences using convolutional neural network," *Pattern Recognit. Lett.*, vol. 129, pp. 115–122, 2020.
31. S. Iqbal, M. U. Ghani, T. Saba, and A. Rehman, "Brain tumor segmentation in multi-spectral MRI using convolutional neural networks (CNN)," *Microsc. Res. Tech.*, vol. 81, no. 4, pp. 419–427, 2018.
32. J. Amin, M. Sharif, M. Yasmin, and S. L. Fernandes, "A distinctive approach in brain tumor detection and classification using MRI," *Pattern Recognit. Lett.*, vol. 0, pp. 1–10, 2017.
33. R. Lavanyadevi, M. MacHakowsalya, J. Nivethitha, and A. Niranjil Kumar, "Brain tumor classification and segmentation in MRI images using PNN," *Proc. - 2017 IEEE Int. Conf. Electr. Instrum. Commun. Eng. ICEICE 2017*, vol. 2017–Decem, pp. 1–6, 2017.
34. A. R. Mathew and P. B. Anto, "Tumor detection and classification of MRI brain image using wavelet transform and SVM," *Proc. IEEE Int. Conf. Signal Process. Commun. ICSPC 2017*, vol. 2018–Janua, no. July, pp. 75–78, 2018.
35. A. Minz, "MR Image classification using adaboost for brain tumor type.2017 IEEE 7th International Advance Computing Conference (IACC)," pp. 701–705, 2017.
36. S. E. Grigorescu, N. Petkov, and P. Kruizinga, "Comparison of texture features based on Gabor filters," *IEEE Trans. Image Process.*, vol. 11, no. 10, pp. 1160–1167, 2002.
37. G. Yadav, S. Maheshwari, and A. Agarwal, "Contrast limited adaptive histogram equalization based enhancement for real time video system," in *Proceedings of the 2014 International Conference on Advances in Computing, Communications and Informatics, ICACCI 2014*, 2014, pp. 2392–2397.
38. J. C. Bezdek, R. Ehrlich, and W. Full, "FCM: The fuzzy c-means clustering algorithm," *Comput. Geosci.*, vol. 10, no. 2–3, pp. 191–203, 1984.
39. N. Otsu, "Threshold Selection Method From Gray-Level Histograms.," *IEEE Trans Syst Man Cybern*, vol. SMC-9, no. 1, pp. 62–66, 1979.
40. X. Zhang, J. Cui, W. Wang, and C. Lin, "A study for texture feature extraction of high-resolution satellite images based on a direction measure and gray level co-occurrence matrix fusion algorithm," *Sensors (Switzerland)*, vol. 17, no. 7, 2017.
41. T. O. KvÅlseth, "Entropy and Correlation: Some Comments," *IEEE Trans. Syst. Man Cybern.*, vol. 17, no. 3, pp. 517–519, 1987.
42. W. Huang and Z. Jing, "Evaluation of focus measures in multi-focus image fusion," *Pattern Recognit. Lett.*, vol. 28, no. 4, pp. 493–500, 2007.
43. Z. Wang, A. C. Bovik, H. R. Sheikh, and E. P. Simoncelli, "Image quality assessment: From error visibility to structural similarity," *IEEE Trans. Image Process.*, vol. 13, no. 4, pp. 600–612, 2004.